Available online at www.sciencedirect.com
SCIENCE DIRECT
Journal of Power Sources 156 (2006) 448–454
JOURNAL OF POWER SOURCES
www.elsevier.com/locate/jpowsour

Analysis and minimization of input ripple current in PWM inverters for designing reliable fuel cell power systems

Wajiha Shireen [a,*], Rahul A. Kulkarni [a], M. Arefeen [b]

[a] *University of Houston, Houston, TX 77204-4022, USA*
[b] *Texas Instruments Inc., 12203 Southwest Freeway, TX, USA*

Received 19 May 2005; accepted 9 June 2005
Available online 10 August 2005

Abstract

This paper presents the implementation of a technique to minimize the input ripple current in three-phase voltage-source pulse width modulated (PWM) inverters when supplying unbalanced/nonlinear loads. This is achieved without increasing the KVA ratings of the dc-link filter components. The results presented are particularly important for designers of fuel cell power systems. Inverter input ripple current has been reported to possibly degrade fuel cell performance and reduce operating life if ripple currents are not adequately controlled. Experimental results from a prototype are included to verify the findings from the analysis and simulation.

Keywords: Fuel cell inverter; Input ripple current compensation

1. Introduction

Fuel cell systems are being considered for utility power applications or for on-site generation for domestic/industrial use [1,2]. One complication is that fuel cells generate direct current (dc) while the electric power system and thus existing end use equipment has been designed for alternating current (ac). Therefore, the fuel cell associated power electronics system must include a dc to ac converter (inverter). Inverter input ripple current has been reported to possibly degrade fuel cell performance and reduce operating life if ripple currents are not adequately controlled [3,4]. Since the reactant utilization is known to impact the mechanical nature of a fuel cell, it is suggested in Ref. [3] that the varying reactant conditions surrounding the cell (due to ripple current) govern, at least in part, the lifetime of the cells. In Ref. [4], it has been shown experimentally that the ripple current can contribute to a reduction in the fuel cell available output power, cause internal losses and increase distortion of its terminal voltage. Passive filters (inductor and/or capacitor) are typically specified to reduce ripple currents in the dc-link between the fuel cell and the inverter to "perceived" low risk values. In order to meet the system requirements, the common practice is to use conservative passive filters in the dc-link that are bulky, expensive and inherently unreliable. In a recent paper, the authors have focused on developing an equivalent circuit model of a fuel cell to evaluate the effects of inverter input ripple current on the performance of a fuel stack [4].

Advanced pulse width modulation (PWM) techniques are used to control the semiconductor switching devices in fuel cell inverters, in order to meet the output voltage and frequency specifications [5,6]. Most advanced PWM methods used for inverter control ensure minimum harmonics at the output. The inverter input current ripple and input power factor have also been a point of concern and various approaches have been proposed so that the total harmonic distortion (THD) of the inverter input current can be kept within the

* Corresponding author.
E-mail addresses: wshireen@uh.edu (W. Shireen), arefeen@ieee.org (M. Arefeen).

0378-7753/$ – see front matter © 2005 Elsevier B.V. All rights reserved.
doi:10.1016/j.jpowsour.2005.06.012

desired limit in accordance to the IEEE 519 standards [7–10]. The approaches in Refs. [10,11] consider balanced and linear three-phase loads. However, a large majority of new loads are nonlinear in nature. Also, single-phase loads connected to a three-phase system in most cases result in unbalanced load conditions.

In view of this, this paper presents the analysis of a three-phase PWM inverter system focusing on assessment of the inverter input current with balanced, unbalanced and nonlinear loads. Analytical equations using the switching function approach are used to find the proper state equations to describe the power conversion circuit in MATLAB [12]. Recent research has shown that the switching function concept is a powerful tool in the analysis of static power converters [13]. In this paper, the switching function approach used to derive the state equations is described and simulation results from the MATLAB program are presented. Effects of balanced, unbalanced and nonlinear loads on the inverter input current are presented. It is found that unbalanced linear or nonlinear loads at the output contribute to the appearance low frequency ripple component in the inverter input current. These ripple currents must be supplied from the dc-link, which necessitates an increase in the KVA ratings of the dc-link filter components. Based on the analytical findings, a modified PWM method is proposed to minimize the lower order ripple currents at the inverter input due to unbalanced load currents without increasing the KVA rating of the dc-link filter capacitor. The proposed method requires sensing of the load currents and balancing out the power in the three phases even when the loads are unbalanced by modifying the inverter modulation in small steps. Experimental results are included to verify the findings from the analysis and simulation.

Reliability and cost of the power electronics system are important considerations for the commercialization of fuel cell power sources. Inverter input ripple current has been reported to possibly degrade fuel cell performance and reduce operating life. The analytical method and proposed ripple minimization technique will enable fuel cell system designers to incorporate more reliable power electronics in their design by taking into account inverter ripple current due to modern nonlinear/unbalanced loads.

2. Analysis of three-phase PWM inverters—the switching function approach

Fig. 1 shows a typical three-phase PWM inverter system. The dc-input for the three-phase inverter is obtained by rectifying a 60 Hz ac source by means of a diode rectifier. The dc-link filter capacitor are so selected that the voltage V_{dc} at the inverter input is constant and ripple-free. The semiconductor switching devices (S_1–S_6) of the inverter are controlled by PWM signals to obtain three-phase near sinusoidal ac voltages of the desired magnitude and frequency at the inverter output.

In order to analyze the PWM inverter system, it is important to compute a dependent variable (input current and output voltage) in terms of an independent variable (input voltage and output current). The switching function approach is used to develop a functional model of the inverter that can be easily simulated in MATLAB.

For a three-phase inverter, the transfer function (T) is composed of three independent switching functions and is given by,

$$T = [S_{a-1} S_{b-1} S_{c-1}] \tag{1}$$

The switching functions are Fourier series representation of the switching sequence used for PWM control of the inverter switching devices. Mathematical representation of

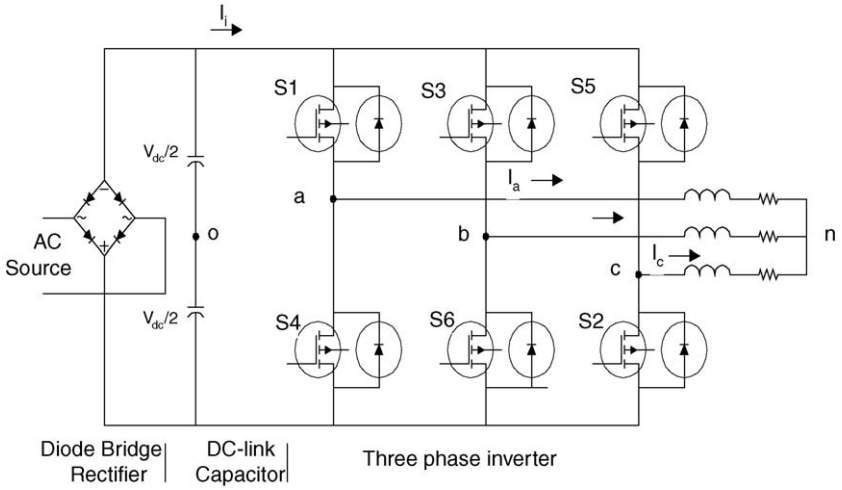

Fig. 1. Three-phase PWM inverter system.

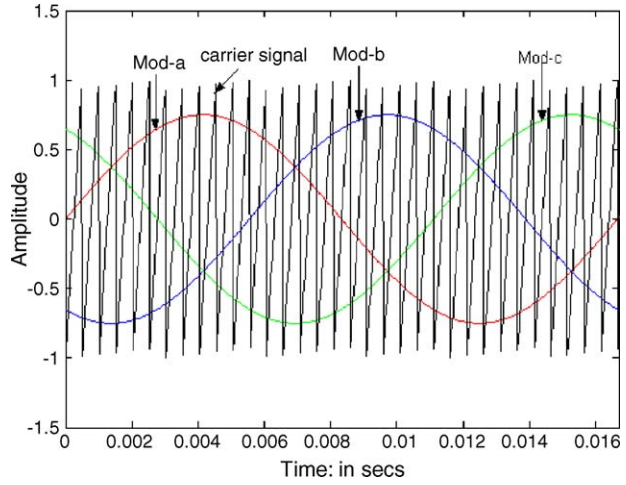

Fig. 2. SPWM generation.

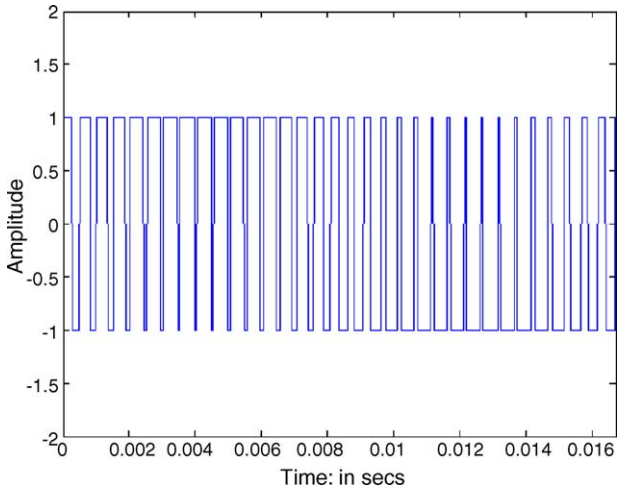

Fig. 3. Switching function S_{a-1}.

the switching functions are given by,

$$S_{a-1}(\omega t) = \sum_{n=1}^{\infty} A_n \sin(n\omega t), \quad S_{b-1}(\omega t) = S_{a-1}\left(\omega t - \frac{2\pi}{3}\right), \quad S_{c-1}(\omega t) = S_{a-1}\left(\omega t + \frac{2\pi}{3}\right) \tag{2}$$

The above switching functions can be generated by using the sinusoidal pulse width modulation (SPWM) technique as shown in Fig. 2. The 'saw tooth' function in MATLAB was used to generate the carrier signal of the desired frequency. The carrier signal frequency used for the simulation was 1980 Hz. The switching function S_{a-1} for phase 'a' of the inverter was generated by comparing the carrier signal with modulating signal Mod_a. Similarly, switching functions S_{b-1} and S_{c-1} can be obtained by comparing carrier signal with modulating signals Mod_b and Mod_c for phases 'b' and 'c', respectively. Fig. 3 shows the switching function S_{a-1}. The frequency spectrum of any periodic signal can be obtained by using the fast Fourier transform (FFT) function in MATLAB. It can be seen from Fig. 4 that the switching function consists of the fundamental 60 Hz component and higher order switching frequency harmonics. Lower order harmonics up to the 33rd (1980 Hz) has been eliminated by the SPWM strategy.

The switching functions S_{a-1}, S_{b-1} and S_{c-1} are used to calculate the inverter output voltages. The voltages v_{ao}, v_{bo} and v_{co} can be obtained as,

$$[v_{ao} v_{bo} v_{co}] = \left(\frac{V_{dc}}{2}\right) T \tag{3}$$

where, V_{dc} is the inverter input voltage. Also,

$$v_{no} = \frac{(v_{ao} + v_{bo} + v_{co})}{3} \tag{4}$$

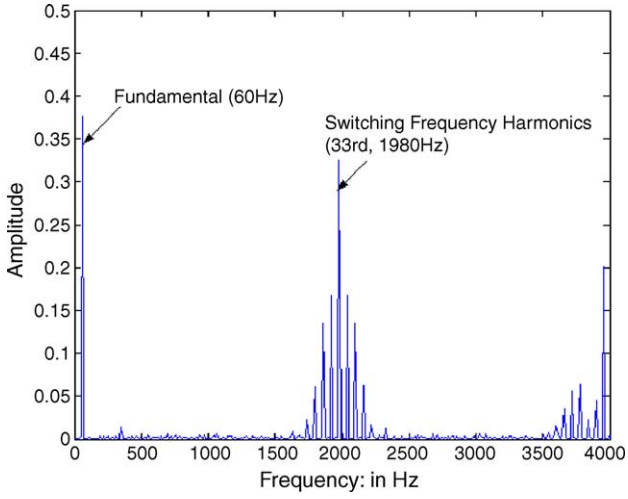

Fig. 4. Frequency spectrum of S_{a-1}.

Hence, assuming star connected loads at the output of the inverter, the inverter line to neutral output voltages are given by,

$$v_{an} = v_{ao} - v_{no}, \quad v_{bn} = v_{bo} - v_{no}, \quad v_{cn} = v_{co} - v_{bo}. \tag{5}$$

3. Analysis of input current ripple using MATLAB

For a given load condition, the inverter input current can be calculated by using another set of three-phase switching functions S_{a-2}, S_{b-2} and S_{c-2}. The switching function S_{a-2} is similar to S_{a-1}, the only difference is that S_{a-1} varies from −1 to +1, whereas S_{a-2} varies between 0 and +1. The frequency spectrum for S_{a-2} will be similar to S_{a-1} (in Eq. (2)) with an additional dc component. The inverter input current I_i can be

calculated as,

$$I_i(\omega t) = I_a(\omega t)S_{a-2} + I_b(\omega t)S_{b-2} + I_c(\omega t)S_{c-2} \quad (6)$$

where, $I_a(\omega t)$, $I_b(\omega t)$ and $I_c(\omega t)$ are the three-phase load currents.

3.1. Inverter input current with balanced linear load

If balanced three-phase linear loads of impedance $Z(\omega)$ are connected at the inverter output, then the inverter output line currents can be computed as,

$$I_a(\omega t) = \frac{v_{an}(\omega t)}{Z(\omega)},$$
$$I_b(\omega t) = I_a\left(\omega t - \frac{2\pi}{3}\right), \quad (7)$$
$$I_c(\omega t) = I_a\left(\omega t + \frac{2\pi}{3}\right)$$

The mathematical operation in Eqs. (6) and (7) were performed in MATLAB to obtain the inverter input current for balanced loads and its corresponding frequency spectrum is shown in Fig. 5. From Fig. 5, it can be seen that the inverter input current (I_i) with balanced loads consists of a dc component and higher order switching frequency harmonics (1980 Hz and above).

3.2. Inverter input current with unbalanced linear load

If three-phase unbalanced loads $Z_a(\omega)$, $Z_b(\omega)$ and $Z_c(\omega)$ are connected at the inverter output, using the voltages from Eq. (5), the three-phase unbalanced currents can be calculated as,

$$I_a(\omega t) = \frac{v_{an}(\omega t)}{Z_a},$$
$$I_b(\omega t) = \frac{v_{bn}(\omega t)}{Z_b}, \quad (8)$$
$$I_c(\omega t) = \frac{v_{cn}(\omega t)}{Z_c}$$

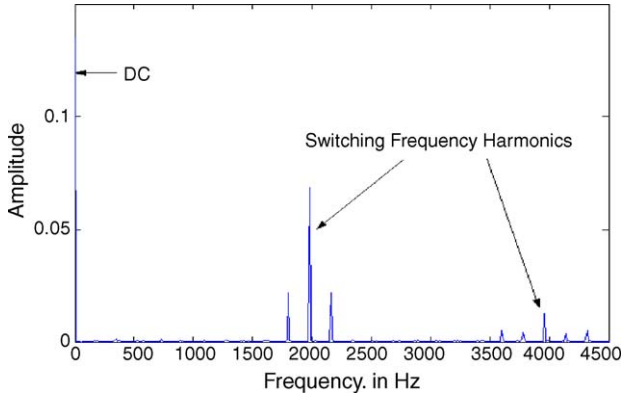

Fig. 5. FFT of I_i with balanced load.

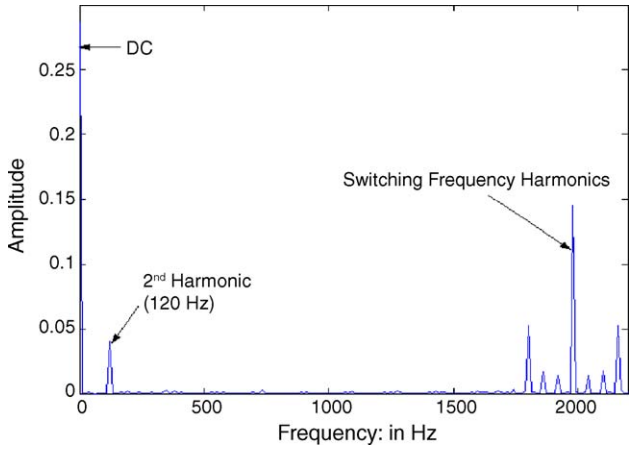

Fig. 6. FFT of I_i with unbalanced load.

The same approach used for balanced loads can be used to plot the inverter input current. Fig. 6 illustrates the FFT of the inverter input current with unbalanced loads. It can be seen that in addition to the dc component, the inverter input current consists of 120 Hz component of significant magnitude. Hence, unbalanced linear loads at the inverter output generate abnormal lower order harmonics at the inverter input which are not present in the case of balanced loads.

3.3. Inverter input current with balanced nonlinear load

When loads connected at the output of the inverter are nonlinear in nature, the load currents consists of harmonics in addition to the fundamental frequency component. Assuming the following balanced but nonlinear load currents are assumed for inverter input current calculation.

$$I_a(\omega t) = \sum_{n=1,3,5,7,9} I_n \sin(n\omega t - \theta_n),$$
$$I_b(\omega t) = I_a\left(\omega t - \frac{2\pi}{3}\right), \quad (9)$$
$$I_c(\omega t) = I_a\left(\omega t + \frac{2\pi}{3}\right)$$

Using Eq. (6), the inverter input current was calculated. The FFT of the input current showed the appearance of lower harmonics (6th, 12th, etc.) in addition to the dc component in the inverter input current spectrum. But, these harmonics are very small in magnitude. Hence, balanced nonlinear loads at the inverter output do not produce any significant lower order harmonics at the inverter input.

3.4. Inverter input current with unbalanced nonlinear load

Fig. 7 shows the FFT of I_i with unbalanced nonlinear loads at the inverter output. Note the appearance of all the abnormal lower order harmonics (2nd, 4th, 5th, etc.). Hence, unbalanced nonlinear loads at the inverter output generate abnormal lower order harmonics at the inverter input.

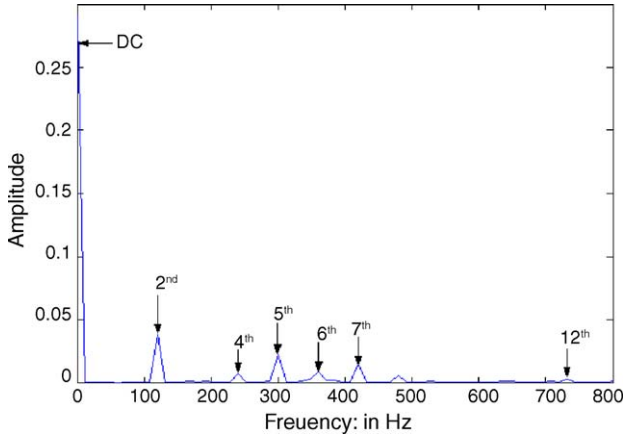

Fig. 7. FFT of I_i with unbalanced nonlinear load.

4. Minimization of input ripple current

It is evident from the analysis presented in the earlier sections that the inverter input current contains low frequency ripple components if unbalanced/nonlinear loads are connected at the inverter output. As discussed in Section 1, these abnormal harmonics must be supplied from the dc-link, which necessitates an increase in the KVA ratings of the dc-link filter components. In this section, a ripple minimization technique is proposed which does not necessitate the increase in dc-link filter values even with unbalanced loads at the inverter output.

The three-phase switching functions S_{a-2}, S_{b-2} and S_{c-2} mentioned in Section 3 can be mathematically represented as,

$$\begin{aligned} S_{a-2}(\omega t) &= A_0 + \sum_{n=1}^{\infty} A_n \sin(n(\omega t + \theta_a)), \\ S_{b-2}(\omega t) &= A_0 + \sum_{n=1}^{\infty} A_n \sin\left(n\left(\omega t - \frac{2\pi}{3} + \theta_b\right)\right), \\ S_{c-2}(\omega t) &= A_0 + \sum_{n=1}^{\infty} A_n \sin\left(n\left(\omega t + \frac{2\pi}{3} + \theta_c\right)\right) \end{aligned} \quad (10)$$

where, θ_a, θ_b and θ_c are phase shifts in the three-phase modulating signals. Under normal balanced conditions, $\theta_a = \theta_b = \theta_c = 0$.

Let the three-phase output currents of the inverter be,

$$\begin{aligned} I_a(\omega t) &= I_a \sin(\omega t - \theta_{\text{load}-a}), \\ I_b(\omega t) &= I_b \sin\left(\omega t - \frac{2\pi}{3} - \theta_{\text{load}-b}\right) \\ I_c(\omega t) &= I_c \sin\left(\omega t + \frac{2\pi}{3} - \theta_{\text{load}-c}\right) \end{aligned} \quad (11)$$

where, $\theta_{\text{load}-a}$, $\theta_{\text{load}-b}$ and $\theta_{\text{load}-c}$ represent the impedance angles associated with the three-phase loads.

While calculating the input current using Eq. (6), the product of $I_a(\omega t)$ and S_{a-2} results in harmonic components at frequencies $(n-1)\omega$ and $(n+1)\omega$. We obtain a dc component when $n = 1$, but we also get a second harmonic component of magnitude $I_a A_1$. Similar components are obtained from the products $I_b(\omega t)S_{b-2}$ and $I_c(\omega t)S_{c-2}$. When the loads are balanced, $I_a = I_b = I_c$ and $\theta_{\text{load}-a} = \theta_{\text{load}-b} = \theta_{\text{load}-c}$. Hence, the second harmonic components are also balanced and the sum of the three components adds up to zero. When the load currents are unbalanced, the second harmonic current component obtained from the product terms in Eq. (6) do not add up to zero and that result in the appearance of the second harmonic in the inverter input current. Based on this analysis, the proposed technique involves phase correction and magnitude correction of the modulating signals used for inverter control. This would ensure that sum of the second harmonic components resulting from the three product terms in Eq. (6) add up to zero regardless of the unbalance in the load.

4.1. Phase angle correction

Substituting Eqs. (10) and (11) in Eq. (6) gives the input current expression. Using the input current expression, the phase angle correction that needs to be introduced in the modulating signals of each phase in order to make the second harmonic components in the input current expression balanced is given by,

$$\theta_a = \frac{\theta_{\text{load}-a}}{2}, \quad \theta_b = \frac{\theta_{\text{load}-b}}{2}, \quad \theta_c = \frac{\theta_{\text{load}-c}}{2} \quad (12)$$

4.2. Magnitude correction

The inverter modulation needs to be modified to maintain the equality,

$$M_a I_a = M_b I_b = M_c I_c \quad (13)$$

where, M_a, M_b and M_c are the magnitudes of the modulating signals Mod_a, Mod_b and Mod_c shown in Fig. 2. The following is the step-by-step process to implement the phase and magnitude correction technique:

1. Initially, modulating signals are equal in magnitude and are displaced 120° from each other.
2. Load currents are measured, if they are unbalanced, phase shifts equal to half of the impedance angles are introduced to the modulating signals of the corresponding phase.
3. Load currents are measured and checked for the equality in Eq. (13).
4. M_a, M_b and M_c are changed in small steps, keeping their average value same as that in step [1].
5. Steps [3] and [4] are repeated until the desired equality in step [3] is reached.

Fig. 8 shows the simulated inverter input current with the above technique in effect. Comparing with Fig. 6, it can be seen that the 2nd harmonic component has been reduced to nearly zero.

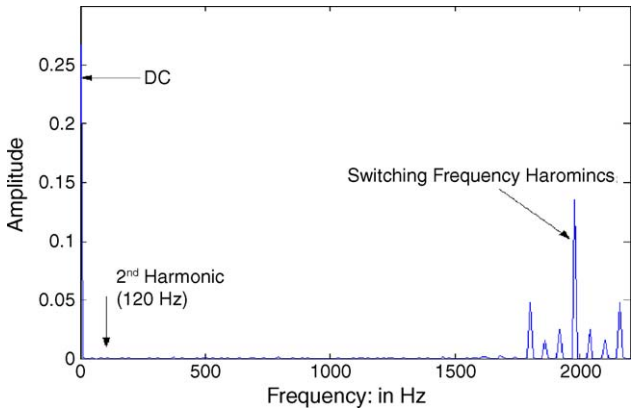

Fig. 8. FFT of I_i with unbalanced load (with correction).

5. Experimental results

A laboratory prototype of a three-phase inverter as shown in Fig. 1 was implemented to verify the findings from the analysis and simulation. The dc-input voltage was set at 50 V. A DSP controller from Texas Instruments C2000 family was used to control the system. The DSP controller provided on-chip PWM modules with multiple PWM outputs. The on-chip 10-bit analog-to-digital converter was utilized for data acquisition to obtain load current information. The 16-bit fixed point DSP core was the computational engine for the implementation of the proposed technique. The PWM switching frequency was set at 20 kHz with a fundamental frequency of 60 Hz. Fig. 9 shows the experimental inverter input current with balanced RL loads. Lamp loads were used as the resistive load. The FFT of the current in Fig. 9 shows the presence of the dc component and higher order normal switching frequency harmonics, which agrees with the simulation results. Then, the inverter prototype was tested with unbalanced RL loads. This was achieved by connecting different number of lamp loads in each phase while keeping the inductor in each

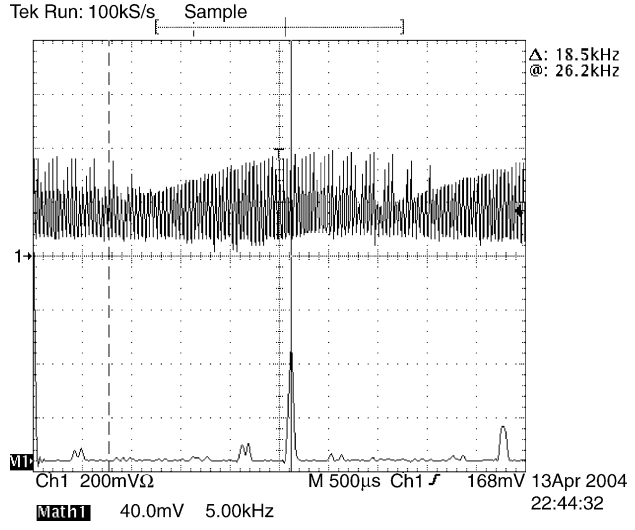

Fig. 9. FFT of I_i with balanced load.

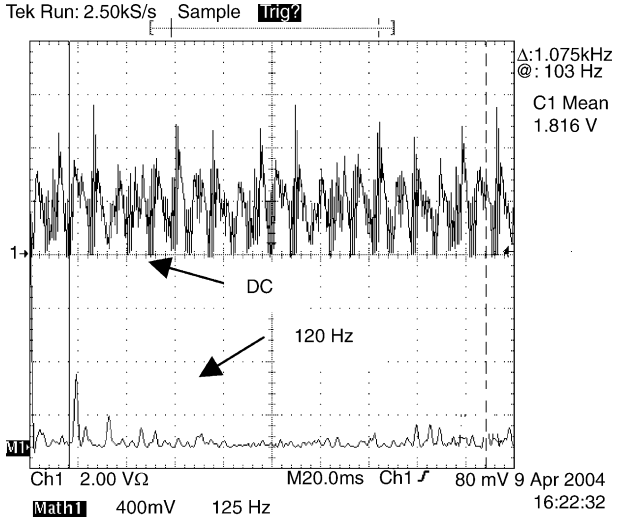

Fig. 10. Experimental I_i and FFT with unbalanced loads (without correction).

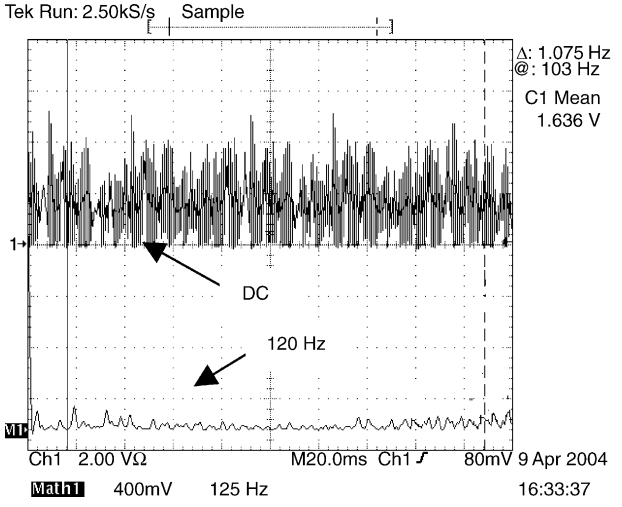

Fig. 11. Experimental I_i and FFT with unbalanced loads (with correction).

phase constant. Fig. 10 shows the experimental inverter input current with unbalanced loads. It can be seen that the input current now consists of a 2nd harmonic (120 Hz) component of significant magnitude (about 30% of the dc component). Fig. 11 shows the inverter input current with the same unbalanced loads (as in Fig. 10) but with the proposed correction technique in effect. It can be seen that the lower order 2nd harmonic (120 Hz) component has been significantly reduced without affecting the dc component of the current.

6. Conclusions

A ripple minimization technique to minimize the input ripple current in three-phase voltage-source pulse width modulated inverters when supplying unbalanced/nonlinear loads is presented. The proposed technique can contribute in improving the reliability and reducing the cost of the

power electronics system in the commercialization of fuel cell power sources. The proposed technique is verified in an actual setup and experimental results are included to verify the findings from analysis and simulation.

References

[1] M.W. Ellis, M.R. Von Spakovsky, D.J. Nelson, Fuel cell systems: efficient, flexible energy conversion for the 21st century, Proceedings of the IEEE 89 (December (12)) (2001) 1808–1818.
[2] M. Farooque, H.C. Maru, Fuel cells—the clean and efficient power generators, Proceedings of the IEEE 89 (December (12)) (2001) 1819–1829.
[3] R. Gemmen, Analysis for the effect of inverter ripple current on fuel cell operating condition, in: Proceedings of the ASME 2001 International Mechanical Engineering Congress and Exposition, New York, NY, 2001.
[4] W. Choi, P. Enjeti, J.W. Howze, G. Juong, An experimental evaluation of the effects of ripple current generated by the power conditioning stage on a proton exchange membrane fuel cell stack, J. Mater. Eng. Perform. 13 (June (3)) (2004) 257–264.
[5] W. Choi, P. Enjeti, J.W. Howze, Development of an equivalent circuit model of a fuel cell to evaluate the effects of inverter ripple current, IEEE Appl. Power Electron. Conf. Rec. v1 (2004) 356–361.
[6] G.A. O'Sullivan, Fuel cell inverters for utility applications, IEEE Annu. Power Electron. Specialists Conf. 3 (2000) 1191–1194.
[7] K.M. Salim, et. al., Development of a fuel cell power conditioner system, Proceedings of the International Conference on Power Electronics and Drive Systems, vol. 2, 1999, pp. 1153–1156.
[8] A.M. El-Tamaly, P.N. Enjeti, Improved approach to reduce harmonics in the utility interface of wind, photovoltaic and fuel cell power systems, Conference Proceedings—IEEE Applied Power Electronics Conference and Exposition-APEC 2 (2000) 1059–1065.
[9] R. Naik, N. Mohan, A novel grid interface for photovoltaic, wind-electric, and fuel cell systems with a controllable power factor of operation, Appl. Power Electron. Conf. (APEC) Conf. Proc. v2 (1995) 995–998.
[10] P.A. Dahono, et al., Analysis and Minimization of ripple components of input current and voltage of PWM inverters, IEEE Trans. Ind. Electron. 32 (July/August (4)) (1996) 945–950.
[11] N.K. Poon, et al., Techniques for input ripple current cancellation: classification and implementation, IEEE Trans. Power Electron. 15 (November (6)) (2000) 1144–1152.
[12] L. Salazar, G. Joos, PSpice simulation of three phase inverter by means of switching function, IEEE Trans. Power Electron. 9 (January (1)) (1994) 35–42.
[13] B.-K. Lee, M. Ehsani, A simplified functional simulation model for three-phase voltage-source inverter using switching function concept, IEEE Trans. Ind. Electron. 48 (April (2)) (2001) 309–321.